

Suppression of miR-21-5p by Ginsenoside Rb1 Prevents Atherosclerosis and Attenuates Endothelial Dysfunction by Inducing KRIT1

Tiangang Zhou

The First Affiliated Hospital of Shandong First Medical University

Dehua Sun

The First Affiliated Hospital of Shandong First Medical University

Yunfeng Hou

the First Affiliated Hospital of Shandong First Medical University

Zhonghui Zhang (✉ zhangzh2412_tetama@hotmail.com)

The First Affiliated Hospital of Shandong First Medical University <https://orcid.org/0000-0002-5100-2714>

Research

Keywords: endothelial dysfunction, ginsenoside Rb1, inflammation, miR-21-5p, KRIT1

Posted Date: April 13th, 2021

DOI: <https://doi.org/10.21203/rs.3.rs-400608/v1>

License:   This work is licensed under a Creative Commons Attribution 4.0 International License.

[Read Full License](#)

Abstract

Background

Endothelial dysfunction (ED) is a risk factor contributing to atherosclerosis (AS)-related complications. MiR-21-5p is a potential therapeutic target for treating ED and can be modulated by ginsenoside Rb1 (Rb1). In the current study, the anti-ED effects of Rb1 were explored by focusing on miR-21-5p/KRIT1 axis.

Methods

ED was induced in rats using high-fatty diet (HFD) method and treated with Rb1. The changes in hemodynamics parameters, blood lipid level, systemic inflammation, and miR-21-5p/KRIT1 axis were detected *in vivo*. Human umbilical vein endothelial cells (HUVECs) were subjected to oxLDL to induce *in vitro* ED model and then handled with Rb1. The role of miR-21-5p in the function of Rb1 was further assessed by inducing its level in HUVECs.

Results

It was shown that the administrations of Rb1 improved hemodynamics parameters, decreased blood lipid levels, and suppressed pro-inflammatory cytokine production in HFD rats, which was associated with the down-regulation of miR-21-5p and the up-regulation of KRIT1. In HUVECs, Rb1 suppressed apoptosis, inhibited inflammation, down-regulated miR-21-5p level, and induced KRIT1 level. The overexpression of miR-21-5p counteracted the protective effects of Rb1 on HUVECs by increasing cell apoptosis and inflammation.

Conclusions

The findings confirmed the protective effects of Rb1 against ED depended on the inhibition of miR-21-5p.

Introduction

Endothelial dysfunction (ED) is a major risk factor in the initiation of cardiovascular disorders (CVDs) (1–3), and is caused by the imbalance between vasodilating and vasoconstricting substances produced by the endothelium (4, 5). The phenotype changes in endothelial cells (ECs) associated with ED are important for the maintenance of vascular homeostasis, and for the regulation of acute and chronic oxidative stress and inflammatory responses in the arteries (6). The failure in the control of ED development always promotes atherosclerosis (AS), which results in the early changes in the natural history of an atherosclerotic lesion (7, 8). Thus, in the recent years, the management of ED progression has been conceived as a promising strategy for preventing the development of AS and CVDs.

Accumulated evidence infers that microRNAs (miRs) play critical roles in affecting the function of ECs. MiRs are highly conserved noncoding single-stranded RNAs (20–26 nucleotides in length) that are involved in the regulation of gene expression in a post-transcription manner. Currently, more than 700 miRs have been identified in human genome and the dys-expression of miRs are reported to be associated with the development of multiple human diseases, including AS, cardiac hypertrophy, arterial hypertension, and inflammatory diseases (9–11). The study by Poliseno et al. showed that the levels of 27 angiogenesis-regulating miRs such as miR-221 and miR-21 were abnormally high in human umbilical vein ECs (HUVECs) (12). The importance of miRs in regulating EC function was further demonstrated by Suárez et al., the authors showed that the silencing of Dicer dramatically affected the expression of several regulators of angiogenesis, such as endothelial cell-specific receptor kinase, vascular endothelial growth factor receptor 2, (eNOS), and interleukin 8, suppressing the proliferation of ECs (13). In our pre-experiment with microarray detections (unpublished data), we have found that the expression of miR-21-5p was substantially induced by the ED. The result was in consistence with the previous reports (12). Moreover, based on TargetscanHuman 7.1 prediction (http://www.targetscan.org/cgi-bin/targetscan/vert_71/view_gene.cgi?rs=ENST00000394507.1&taxid=9606&members=miR-21-5p/590-5p&showcnc=0&shownc=0&subset=1), one of the downstream effectors of miR-21-5p, KRIT1, plays central role in maintaining the function of ECs (6). Thus, the current study selected miR-21-5p/KIRT1 axis as the potential target for handling ED.

In the recent years, the exploration of active components from Traditional Chinese Medicine (TCM) for treatments of different chronic disorders has drawn a lot of interests and achieved considerable outcomes. Ginseng, the root of *Panax ginseng* ca Meyer, is one of the most famous herbs in TCM and has been used for promoting human health for centuries (14, 15). Regarding its effects on EC function, the study by Xie showed that ginsenoside Re attenuated high glucose-induced retinal EC injuries by inhibiting HIF-1 α /VEGF signaling transduction (16), and the study by Geng et al. showed that ginsenoside Rg3 alleviated oxLDL-induced ED by regulating PPAR γ /FAK signaling pathway (17). Ginsenoside Rb1 (Rb1) is another active component isolated from ginseng. The compound has various biological activities including antioxidative stress, anti-obesity, and anti-inflammation (18–20). The study by Zheng et al. implied that Rb could reduce H₂O₂-induced ED by activating sirtuin-1/AMPK pathway (21), and thus can be employed as a treatment agent for restoring EC function. Moreover, Rb1 had shown its protective effects on cardiomyocytes by inhibiting the level of miR-21 (22), representing the critical role of the miR in the functioning of Rb1. Thus, in the current study, we hypothesized that the EC protective effects of Rb1 were also related to its interaction with miR-21-5p.

To verify the hypothesis, rats were subjected to high-fatty diet (HFD) model to induce EC injuries *in vivo* and the then treated with Rb1. Then human umbilical vein endothelial cells (HUVECs) were incubated with oxLDL and Rb1 to explore the potential mechanism in the EC protective effects of Rb1.

Methods

High-fatty diet (HFD) model and Rb1 administration

All the animal experiments were performed following the accepted principles for laboratory animal use and care as found in for example the European Community guidelines with the approval of the Ethics Committee of the First Affiliated Hospital of Shandong First Medical University. Six-week-old male Sprague Dawley (SD) rats (180-200 g) were purchased from Beijing HFK Bioscience Co., Ltd. (Beijing, China) and housed individually under 12-h light/dark cycle with *ad libitum* to water. To assess the effects of Rb1 on endothelium injures, 12 rats were randomly divided into four groups (three for each group): Control group, rats fed with a standard chow diet (24% protein, 66% carbohydrates, and 10% fat) for ten weeks; HFD group, rats fed with a HFD (20% protein, 20% carbohydrates, and 60% fat) for ten weeks; HFD + L group, rats subjected to HFD model and the diet containing low dose of Rb1 (20 mg/kg body weight) (Victory, Sichuan, China); HFD + H group, rats subjected to HFD model and the diet containing low dose of Rb1 (40 mg/kg body weight).

Detection of hemodynamics parameters

Upon completion of the experiments, the changes in hemodynamics parameters of model rats, including interventricular septal thickness (IVS), left ventricular posterior wall thickness (LVPW), aortic diameter (AO), left ventricular internal diameter (LV), and right atrium diameter (RV) were measured using the algorithms of ultrasound system using Philips iE33 system (Philips Ultrasound, Bothell, WA). Then rats were sacrificed with i.p. injection of overdose (200 mg/kg body weight) pentobarbital sodium, and the abdominal aorta tissues and blood samples were collected for subsequent detections.

Detection of blood lipids and cytokines

The blood levels of lipid species, including total cholesterol (TC), high-density lipoprotein (HDL), low density lipoprotein (LDL), and triglyceride were measured following the previously described method (23). The blood levels of cytokines, including IL-6 (H007, Nanjing Jiancheng Bioengineering Institute, China), IL-1 β (H002, Nanjing Jiancheng Bioengineering Institute, China), and TNF- α (H052, Nanjing Jiancheng Bioengineering Institute, China), were measured using corresponding ELISA kits following the procedures in the manufacturers' instructions.

Detection of miR-21-5p/KIRT1 axis activity

Total RNA was extracted using Trizol method and cDNA templates were achieved from RNA using M-MLV according to the manufacturer's instruction. The relative expression levels of different genes (miR-21-5p, forward: 5'-CGGCGGTAGCTTATCAGACTGA-3', reverse: 5'-ATCCAGTGCAGGGTCCGAGG-3'; U6, forward: 5'-AGAGAAGATTAGCATGGCCCCTG-3', reverse: 5'-ATCCAGTGCAGGGTCCGAGG-3') were detected using ExicyclerTM 96 (BIONEER, South Korea) and calculated according to the formula of $2^{-\Delta\Delta ct}$.

Total protein was extracted using the RIPA lysis buffer and was subjected to sodium dodecyl sulfate polyacrylamide gel electrophoresis (SDS-PAGE). The membranes were firstly incubated with primary antibodies, including KIRT1 (1:500) (ab196025, Abcam, USA) and GAPDH (1:1000) (ab8245, Abcam, USA), at 4°C overnight and then with secondary IgG-HRP antibodies at 37°C for 45 min. Protein blots were

developed using Beyo ECL Plus reagent (P0018, Beyotime Biotechnology, China) and the images were scanned in the Gel Imaging System (WD-9413B, Liuyi Factory, China). The relative expression levels of the different proteins were calculated based on the data of integrated optical density measured with Gel-Pro-Analyzer (Media Cybernetics, USA).

Cell culture and treatments

HUVECs were purchased from Wuhan Procell Life Science and Technology and cultured in endothelial cell culture medium (Ham's F-12K) supplemented with 10% fetal bovine serum (FBS) in an atmosphere consisting of 5% CO₂ at 37°C. To detect the protective effects of Rb1 on HUVECs against ED, the cells were divided into four groups: Control group, healthy HUVECs cultured in a density of 2 × 10⁵ cells/mL. OxLDL group, HUVECs (2 × 10⁵ cells/mL) incubated with oxLDL (Guangzhou Yiyuan Biotechnologies, Guangzhou, China) for 24 h. OxLDL + Rb1 group, HUVECs (2 × 10⁵ cells/mL) incubated with oxLDL (Guangzhou Yiyuan Biotechnologies, Guangzhou, China) and 30 μM Rb1 for for 24 h.

Detection of cell apoptosis

Apoptotic rate in HUVECs was detected using the apoptosis detection kit (KGA106, KeyGEN BioTECH, China): briefly, 5 μl Annexin V was incubated with cells for 10 min at room temperature. Then the cells were resuspended with 1×Binding buffer and added with 5 μl Propidium Iodide (PI). The total apoptotic rate was analyzed using a FACScan flow cytometer (Accuri C6, BD, USA), which was equal to the sum of the late apoptotic rate and the early apoptotic rate.

Modulation of miR-21-5p level

To determine the role miR-21-5p in the protective effects of Rb1 on HUVECs, HUVECs were further transfected with miR-21-5p using Lipofectamine 2000 (Invitrogen, Carlsbad, CA) 24 h before oxLDL and Rb1 (30 μM) treatments. Then the effects of miR-21-5p overexpression on cell apoptosis and inflammation were detected.

Dual luciferase assay

Wild type (WT) and mutant type (MUT) of KRIT1 3'UTR were inserted into pmirGLO plasmid (between NheI and Sal I) to form luciferase vector. Mimics of miR-21-5p (5'-UAGCUUAUCAGACUGAUGUUGA-3') and negative control (NC) mimics (5'-UUCUCCGAACGUGUCACGUTT-3') were used to detect the bind of miR-21-5p to KIRT1 3'UTR. Transfections int HUVECs were performed using Lipofectamine 2000 (Invitrogen, Carlsbad, CA). Luciferase activity of firefly was detected with Luciferase Activity Detection Kit (E1910, Promega, USA) using a Chemiluminescence Apparatus (Lumat LB 9507, Berthold, German).

Statistical analysis

Data were expressed in the format of mean ± standard deviation (SD). One-way analysis of variance (ANOVA) with post-hoc comparisons using Tukey method was performed using Graphpad Prism version

6.0 (GraphPad Software, Inc., San Diego, CA) with a significant level of 0.05 (two-tailed).

Results

Rb1 improved hemodynamics in HFD rats

The development of ED was evaluated by comparing hemodynamics parameters in both healthy and HFD rats. As shown in Figure 1, interventricular septal thickness IVS and LVPW were significantly increased in HFD rats ($P < 0.05$), while AO, LV, and RV were decreased ($P < 0.05$) (Figure 1). After the administration of Rb1, the values of the parameters were restored to levels similar to those in Control groups (Figure 1). The high dose of Rb1 showed stronger improvement effects on hemodynamics parameters, but the difference between low dose and high dose was statistically insignificant.

Rb1 improved blood lipid production and suppressed systemic inflammatory response in HFD rats

The effects of Rb1 on ED were further assessed by measuring the production of blood lipids and cytokines in rats. Regarding blood lipid levels, HFD administration increased the production of TC, LDL, and triglyceride, while the suppressed the production of HDL (Figure 2). After the administrations of Rb1, the levels of blood lipids were restored, which was within similar ranges as those in Control group. The administration of Rb1 also suppressed the production of pro-inflammatory response cytokines in HFD rats, the levels of IL-6, IL-1 β , and TNF- α were all increased in blood samples of HFD rats and then inhibited by Rb1 administrations (Figure 3). The detection of blood lipids and cytokines confirmed the induction of ED in HFD rats and the protective effects of Rb1 against ED-associated symptoms. However, the two Rb1 doses showed no significant difference in improve blood lipid levels and cytokine production, which was identical with the its effects on hemodynamics parameters (Figure 2 and Figure 3).

Rb1 inhibited miR-21-5p level and induced KRIT1 in HFD rats

The changes in miR-21-5p/KRIT1 axis under Rb1 administrations were also detected. The induction of ED up-regulated the expression of miR-21-5p (Figure 4A). Correspondingly, the downstream effector of miR-21-5p, KRIT1, was down-regulated (Figure 4B). However, in rats administrated with Rb1, the expression of miR-21-5p was inhibited, while the expression of KRTI1 was induced (Figure 4). Given the changes in miR-21-5p/KRIT1 axis was synchronized with the changes in phenotypes, it might infer that the effects of Rb1 against ED were associated with the function of miR-21-5p/KRIT1 axis.

Rb1 inhibited miR-21-5p level and induced KRIT1 level in oxLDL-treated HUVECs, which contributed to the suppressed apoptosis and inflammatory response

The potential mechanism driving the effects of Rb1 on ED was further explored with ox-LDL-treated HUVECs. As shown Figure 5A, the expression level of miR-21-5p in HUVECs treated with oxLDL was significantly higher than that in healthy HUVECs, while the expression of KIRT1 was significantly lower ($P < 0.05$) (Figure 5B). The changes in miR-21-5p/KRIT1 axis was associated with the induced apoptosis (Figure 5C) and increased production of cytokines (Figure 5D-5F) in HUVECs. After the treatment of Rb1,

the expression levels of miR-21-5p and KRIT1 were reversed (Figure 5A and Figure 5B), which was in consistence with *in vivo* assays. The reversed activity of miR-21-5p/KRIT1 contributed to the suppressed apoptosis and inflammatory response in HUVECs, further supporting the key role of miR-21-5p/axis in the function of Rb1 against ED.

Rb1 exerted its anti-ED function in a miR-21-5p-inhibition dependent manner

To further explore the role of miR-21-5p in the anti-ED function of Rb1, the level of the miR-21-5p was induced in Rb1-treated HUVECs (Figure 6A). The increased the level of miR-21-5p inhibited the expression of KRIT1 (Figure 6B), induced apoptosis (Figure 6C), and increased the production of IL-6, IL-1 β , and TNF- α (Figure 6D-6F) even under the treatment of Rb1. In addition, the possible regulatory effect of miR-21-5p on KRIT1 was validated in HUVECs: only the co-transfection of miR-21-5p mimic and WT 3'UTR would lead the suppressed fluorescence intensity of luciferase (Figure S1), indicating the specific and direct binding of miR-21-5p to the 3'UTR region of KRIT1 gene. Collectively, the protective effects of Rb1 against ED depended on the inhibition of miR-21-5p, which would activate the transcription of KRIT1 gene directly and improve the physiological condition of endothelium.

Discussion

ED is a crucial pathological alteration contributing to the onset and progression of AS, and is one of the leading mortality- and morbidity- related factors worldwide (24). The management of the early ED is now conceived as a promising strategy for treating AS and related complications. Accumulating evidence demonstrates that natural products from TCM hold great therapeutic potentials for handling ED (25–27). For example, Yang et al. showed that dihydromyricetin attenuated TNF- α -Induced ED by modulating miR-21-mediated DDAH1/ADMA/NO signaling transduction (28). *Panax notoginseng* has a long history as a botanical drug in eastern countries and *Panax notoginseng* saponins (PNS) has been recognized as the major active components contributing the diverse biological functions of *Panax notoginseng*. Additionally, different types of PNS all showed considerable protective effects against ED-induced physiological disorders. In the study by Geng et al., the authors showed that ginsenoside Rg3 Alleviates oxLDL-induced ED by regulating PPAR γ /FAK signaling pathway (17). In another study performed by Xie et al., it was found that ginsenoside Re ameliorated high glucose-induced RF/6A cell injuries by inhibiting HIF-1 α /VEGF pathway (16). In the current study, we employed Rb1 as the protective agent on endothelium against ED both *in vivo* and *in vitro*. Our results showed the administration improved hemodynamics and suppressed systemic inflammatory response in HFD rats, and inhibited cell apoptosis and production of cytokines in oxLDL-treated HUVECs. The data solidly supported the anti-ED function of ginsenosides reported by the previous studies (19, 21). Based on these previous studies, Rb1 could protect ECs against H₂O₂- or oxLDL- induced impairments via multi-pronged mechanisms. For instance, Rb1 could increase SIRT1 level and subsequently suppress Beclin-1 acetylation. Moreover, the induced level of SIRT1 could also activate AMPK signaling and promote the recovery of EC function. The comprehensive understanding of the mechanisms underlying the anti-ED function of ginsenosides will facilitate the

application of the agents in clinic. Thus, in the current study, we further explored the factors that might be involved in the protective effects Rb1 on endothelium against ED-induced by different factors.

The dys-expression of miRs has been proved to be involved in the progression of multiple diseases, including AS-related complications. For example, miR-122 has been highlighted as a promising target for decreasing plasma cholesterol in humans (29). MiR-33a dysregulation contributes to AS progression by promoting lipid build-up and cholesterol retention by regulating the function of the ATP binding cassette (ABC) transporter ABCA1 (30). Regarding the interaction between miRs and ED, miR-181a inhibits vascular inflammation by inhibiting NF- κ B signaling pathway (31). MiR-31 is involved in the negative feedback loop that directly inhibits TNF- α -induced E-selectin and ICAM-1 expression (32). Thus, in the previous study, we employed microarray analyses to identify miRs that response to ED and selected miR-21-5p as the potential therapeutic target by Rb1 (unpublished data). The abnormally high expression level of miR-21-5p in oxLDL-treated HUVECs was in consistence with the reports by Poliseno et al. and by Yang et al. that miR-21 was induced in response to ED (27, 33). Based on our assays, the levels of miR-21-5p were induced both *in vivo* and *in vitro* as a biomarker, confirming the involvement of the miR in the development of ED development. To further explain the mechanism mediating the effects of miR-21-5p to promote ED, we also detected the level of KRIT1, a downstream effector of miR-21-5p. The data showed that the expression of KRIT1 was dramatically inhibited by ED induction, which was directly induced by Rb1. It is well-characterized that the deficiency in KRIT1 function will promote aortic ED (6). Moreover, based on the analysis of TargetscanHuman 7.1, other downstream effectors of miR-21-5p include TIMP3, STAG2, Bcl-2, etc., the inhibition of which by miR-21-5p will all contribute to the development of ED (34, 35). Therefore, the inhibition of miR-21-5p by Rb1 would restore the function of KRIT1 and other anti-ED factors, and finally led to the alleviation of ED symptoms. The key role of miR-21-5p inhibition in the anti-ED effects of Rb1 was further verified by inducing the level of the miR-21-5p in HUVECs co-treated with oxLDL and Rb1. It was found that the induction of miR-21-5p level would counteract the protective effects of Rb1 on HUVECs.

Conclusions

Collectively, the current study for the first time connected the anti-ED function of Rb1 with the function of miRs. Based on the results of a series of *in vivo* and *in vitro* detections, we confirmed that the protective effects of Rb1 on endothelium depended on the inhibition of miR-21-5p, which would restore the function of the downstream effectors such as KRIT1. Since multiple anti-ED effectors of miR-21-5p has been identified, the mechanism mediating the function of Rb1 may be complicated and thus, the application of the compound or other ginsenoside-like compounds should depend on careful pre-clinical tests. Our lab will perform more comprehensive analyses in the future to promote the development of ginsenoside-like compounds as potential therapeutic strategies to prevent or even treat ED.

List Of Abbreviations

ED Endothelial dysfunction

CVD cardiovascular disorders

EC endothelial cell

HFD high-fatty diet

AS atherosclerosis

miR microRNA

HUVEC human umbilical vein endothelial cell

Declarations

Ethics approval and consent to participate

All animal experiments were conducted in the accordance with the Institutional Animal Ethics Committee and Animal Care Guidelines for the Care and Use of Laboratory Animals published by the US National Institutes of Health (NIH Publication No. 85–23, revised 1996).

Consent for publication

All named authors have agreed to the publication of the work.

Funding

Not applicable

Acknowledgements

Not applicable

Conflict of interests

The authors disclose no conflict of interest.

Authors' contributions

TGZ and DHS collected and analyzed the data, and wrote the draft. YFH collected the data. ZHZ designed the experiment, revised the draft, and approved the submission.

Availability of data and material

Data will be provided by the corresponding author when requested.

References

1. Quyyumi AA. Endothelial function in health and disease: new insights into the genesis of cardiovascular disease. *Am J Med.* 1998;32S-9S.
2. Tohru M, Hideyuki M, Toshihiko Y, Issei K. Endothelial cell senescence in human atherosclerosis: Role of telomeres in endothelial dysfunction. *J Cardiol.* 2003;41(1):39-40.
3. Barton M. Obesity and aging: determinants of endothelial cell dysfunction and atherosclerosis. *Pflügers Archiv.* 2010;460(5):825-37.
4. oveia J, Stapor P, Carmeliet P. Principles of targeting endothelial cell metabolism to treat angiogenesis and endothelial cell dysfunction in disease. *Embo Mol Med.* 2014;6(9):1105-20.
5. Hainsworth AH, Oommen AT, Bridges LR. Endothelial cells and human cerebral small vessel disease. *Brain Pathol.* 2015;25(1):44-50.
6. Francesco Vieceli Dalla S, Raffaella M, Giorgio A, Francesca F, Saverio Francesco R. KRIT1 Deficiency Promotes Aortic Endothelial Dysfunction. *Int J Mol.* 2019;20(19):4930-.
7. Michael, Gimbrone, Guillermo, García Ca. Endothelial Cell Dysfunction and the Pathobiology of Atherosclerosis. *Circ Res.* 2016.
8. Vaccarezza M, Balla C, Rizzo P. Atherosclerosis as an inflammatory disease: Doubts? No more. *Heart & Vasculature.* 2018;19:1-2.
9. Seeger T, Boon RA. MicroRNAs in cardiovascular ageing. *J Physiol-London.* 2016;594(8).
10. Feinberg MW, Moore KJ. MicroRNA Regulation of Atherosclerosis. *Circ Res.* 2016;118(4):703.
11. Emma LS, Catherine GD, Christina AB, Peter JP, Joanne TMT. MicroRNAs as Therapeutic Targets and Clinical Biomarkers in Atherosclerosis. *J Clin Med.* 2019;8(12).
12. Poliseño L, Tuccoli A, Mariani L, Evangelista M, Citti L, Woods K, et al. MicroRNAs modulate the angiogenic properties of HUVECs. *Blood.* 2006;108(9):3068-71.
13. Suárez Y, Fernández-Hernando C, Pober JS, Sessa WC. Dicer dependent microRNAs regulate gene expression and functions in human endothelial cells. *Circ Res.* 2007;100(8):1164-73.
14. Zhang, Eryun, Yang, Li, Gao, Bo, et al. Notoginsenoside Ft1 Promotes Fibroblast Proliferation via PI3K/Akt/mTOR Signaling Pathway and Benefits Wound Healing in Genetically Diabetic Mices. *J Pharmacol Exp Ther.* 2016.
15. Fan C, Yuan Q, Tang M. Notoginsenoside R1 attenuates high glucose-induced endothelial damage in rat retinal capillary endothelial cells by modulating the intracellular redox state. *Drug Des Dev Ther.* 2017;11:3343-54.
16. Xie W, Zhou P, Qu M, Dai Z, Zhang X, Zhang C, et al. Ginsenoside Re Attenuates High Glucose-Induced RF/6A Injury via Regulating PI3K/AKT Inhibited HIF-1 α /VEGF Signaling Pathway. *Front Pharmacol.* 2020;11:695.
17. Geng J, Fu W, Yu X, Lu Z, Liu Y, Sun M, et al. Ginsenoside Rg3 Alleviates ox-LDL Induced Endothelial Dysfunction and Prevents Atherosclerosis in ApoE(-/-) Mice by Regulating PPAR γ /FAK Signaling Pathway. *Front Pharmacol.* 2020;11:500.

18. Xiong Y, Shen L, Liu KJ, Tso P, Xiong Y, Wang G, et al. Antiobesity and Antihyperglycemic Effects of Ginsenoside Rb1 in Rats. *Diabetes*. 2010;59(10):2505.
19. Sufang, Chen, Xiang, Li, Yanling, Wang, et al. Ginsenoside Rb1 attenuates intestinal ischemia/reperfusion-induced inflammation and oxidative stress via activation of the PI3K/Akt/Nrf2 signaling pathway. *Mol Med Rep*. 2019.
20. Sun Q, Meng QT, Jiang Y, Liu HM, Lei SQ, Su WT, et al. Protective Effect of Ginsenoside Rb1 against Intestinal Ischemia-Reperfusion Induced Acute Renal Injury in Mice. *Plos One*. 2013;8(12):e80859.
21. Zhenda Z, Min W, Cailian C, Dinghui L, Xiaoxian Q. Ginsenoside Rb1 reduces H2O2-induced HUVEC dysfunction by stimulating the sirtuin-1/AMP-activated protein kinase pathway. *Mol Med Rep*. 2020.
22. Zhang Y, Zhang L, Chu W, Wang B, Zhang J, Zhao M, et al. Tanshinone IIA Inhibits miR-1 Expression through p38 MAPK Signal Pathway in Post-infarction Rat Cardiomyocytes. *Cell Physiol Biochem*. 2010;26(6):991-8.
23. Hayashi T, Jayachandran M, Sumi D, Thakur NK, Esaki T, Muto E, et al. Physiological concentration of 17 β -estradiol retards the progression of severe atherosclerosis induced by a high-cholesterol diet plus balloon catheter injury role of. *Arterioscler Thromb Vasc Biol*. 2000;20(6):9.
24. Peter, Libby, Karin E, Bornfeldt, Alan R, Tall. Atherosclerosis: Successes, Surprises, and Future Challenges. *Circ Res*. 2016.
25. Wang, Hua T, Cai, Xiao J, Shu M, Yuan, et al. Patchouli alcohol attenuates experimental atherosclerosis via inhibiting macrophage infiltration and its inflammatory responses. *Biomed Pharmacother*. 2016.
26. Wang TZ, Chen Y, He YM, Fu XD, Wang Y, Xu YQ, et al. Effects of Chinese herbal medicine Yiqi Huaju Qingli Formula in metabolic syndrome patients with microalbuminuria: a randomized placebo-controlled trial. *J Integr Med*. 2013;11(3):175-83.
27. Tsung Y, Yang, James, Cheng C, Wei, Ming Y, et al. A Randomized, Double-blind, Placebo-controlled Study to Evaluate the Efficacy and Tolerability of Fufang Danshen (*Salvia miltiorrhiza*) as Add-on Antihypertensive Therapy in Taiwanese Patients with Uncontrolled Hypertension. *Phytother Res*. 2011.
28. Yang D, Tan S, Yang Z, Jiang P, Qin C, Yuan Q, et al. Dihydromyricetin Attenuates TNF- α -Induced Endothelial Dysfunction through miR-21-Mediated DDAH1/ADMA/NO Signal Pathway. *BioMed Res Int*. 2018;2018:1-12.
29. Esau C, Davis S, Murray SF, Yu XX, Pandey SK, Pear M, et al. miR-122 regulation of lipid metabolism revealed by in vivo antisense targeting. *Cell Metab*. 2006;3(2):87-98.
30. Jiang H, Zhang J, Du Y, Jia X, Yang F, Si S, et al. microRNA-185 modulates low density lipoprotein receptor expression as a key posttranscriptional regulator. *Atherosclerosis*. 2015;243(2):523-32.
31. Su Y, Yuan J, Zhang F, Lei Q, Zhang T, Li K, et al. MicroRNA-181a-5p and microRNA-181a-3p cooperatively restrict vascular inflammation and atherosclerosis. *Cell Death Dis*. 2019;10(5):365.
32. Yin Y, Li F, Shi J, Li S, Cai J, Jiang Y. MiR-146a Regulates Inflammatory Infiltration by Macrophages in Polymyositis/Dermatomyositis by Targeting TRAF6 and Affecting IL-17/ICAM-1 Pathway. *Cell*

33. Urbich C, Kuehbacher A, Dimmeler S. Role of microRNAs in vascular diseases, inflammation, and angiogenesis. *Cardiovasc Res.* 2008;79(4):581-8.
34. Wang C, Lin Y, Fu Y, Zhang D, Xin Y. MiR-221-3p regulates the microvascular dysfunction in diabetic retinopathy by targeting TIMP3. *Pflugers Archiv.* 2020.
35. Xu D, Guo Y, Liu T, Li S, Sun Y. miR-22 contributes to endosulfan-induced endothelial dysfunction by targeting SRF in HUVECs. *Toxicol Lett.* 2017;269:33-40.

Figures

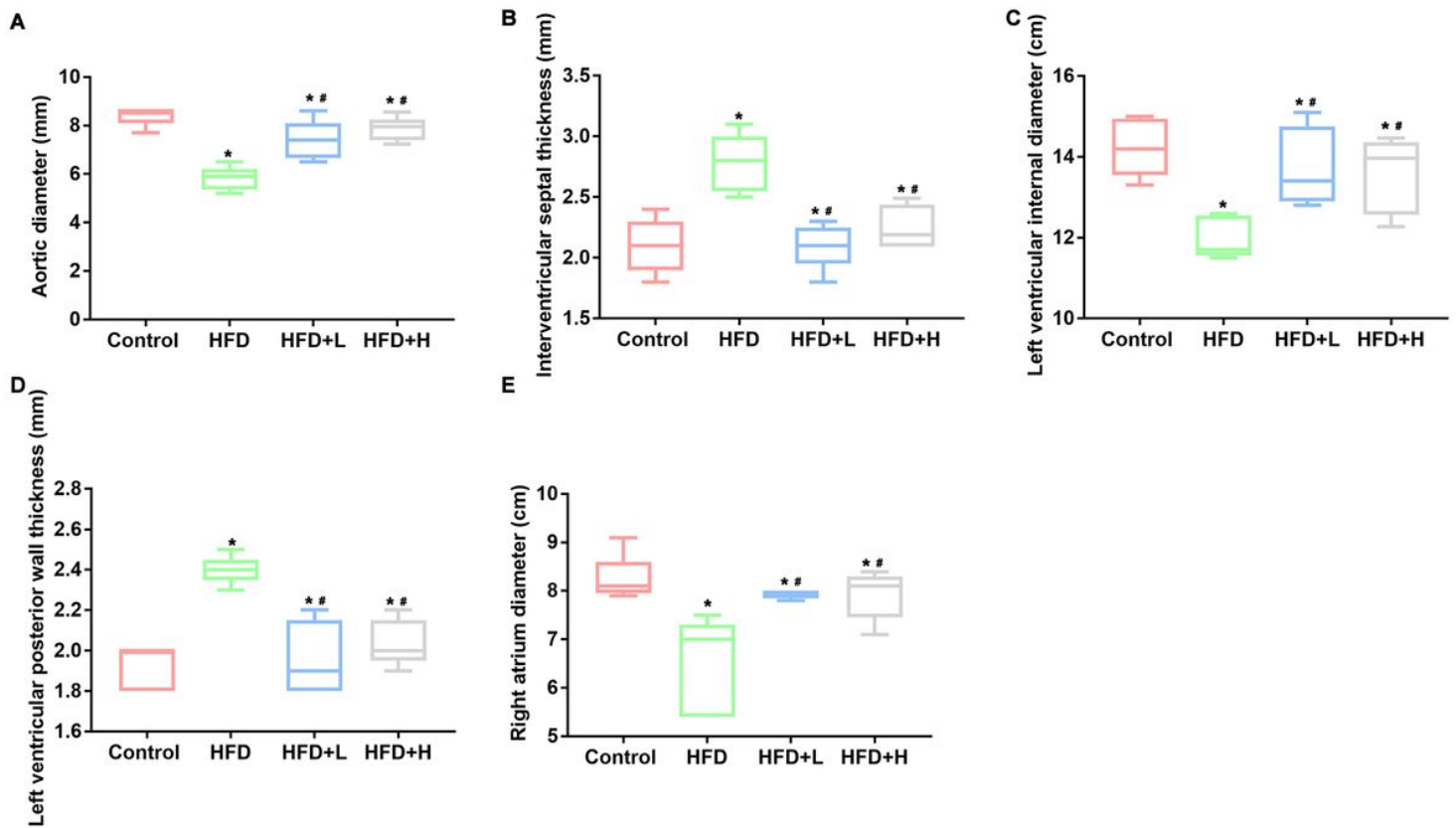


Figure 1

Effects of Rb1 administrations on changes in hemodynamics parameters. HFD rats were administrated with Rb1 of two doses (20 mg/kg BW and 40 mg/kg BW). The levels of AO (A), IVS (B), LV (C), LVPW (D), and RV (E) were then detected. AO, aortic diameter (AO); IVS, interventricular septal thickness; LV, left ventricular internal diameter; LVPW, left ventricular posterior wall thickness; RV, right atrium diameter. “*” represented $P < 0.05$ vs. Control group. “#” represented $P < 0.05$ vs. HFD group. Each parameter was represented by three replicates.

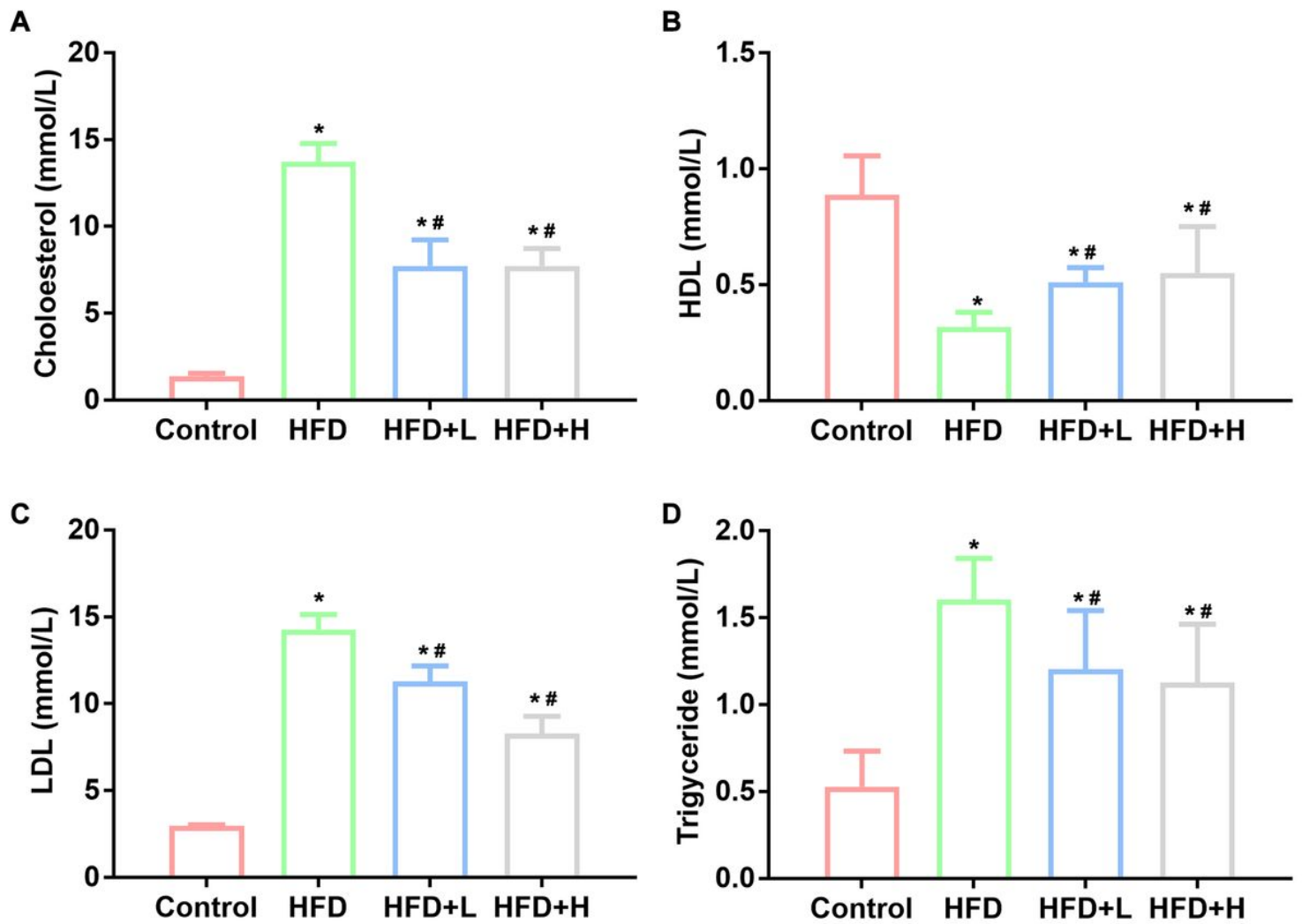


Figure 2

Effects of Rb1 administrations on changes in blood lipid production in HFD rats. HFD rats were administrated with Rb1 of two doses (20 mg/kg BW and 40 mg/kg BW). The production of cholesterol (A), HDL (B), LDL (C), and triglyceride (D) was detected. HDL, high-density lipoprotein; LDL, low density lipoprotein. "*" represented $P < 0.05$ vs. Control group. "#" represented $P < 0.05$ vs. HFD group. Each parameter was represented by three replicates.

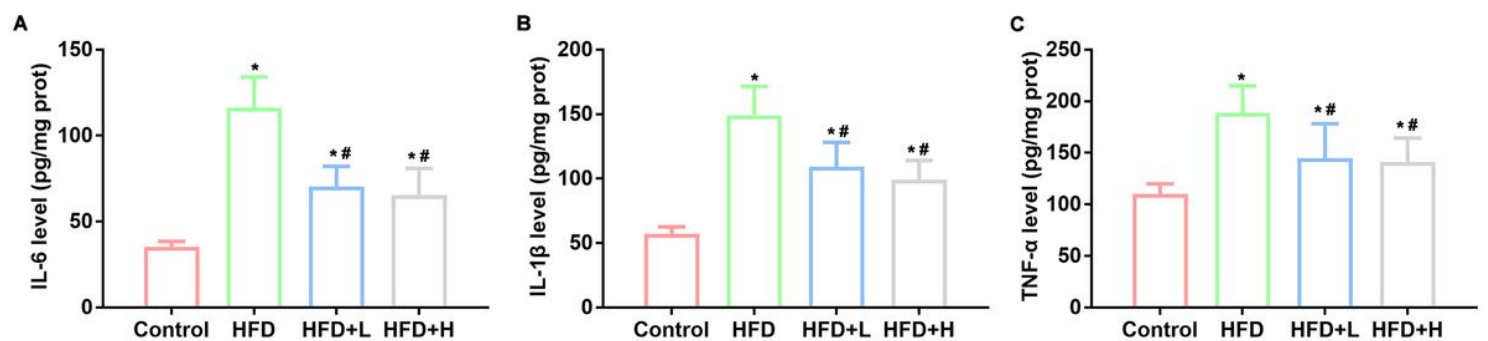


Figure 3

Effects of Rb1 administrations on changes in blood cytokine production in HFD rats. HFD rats were administrated with Rb1 of two doses (20 mg/kg BW and 40 mg/kg BW). The production of IL-6 (A), IL-1 β (B), and TNF- α (C) was detected. "*" represented $P < 0.05$ vs. Control group. "#" represented $P < 0.05$ vs. HFD group. Each parameter was represented by three replicates.

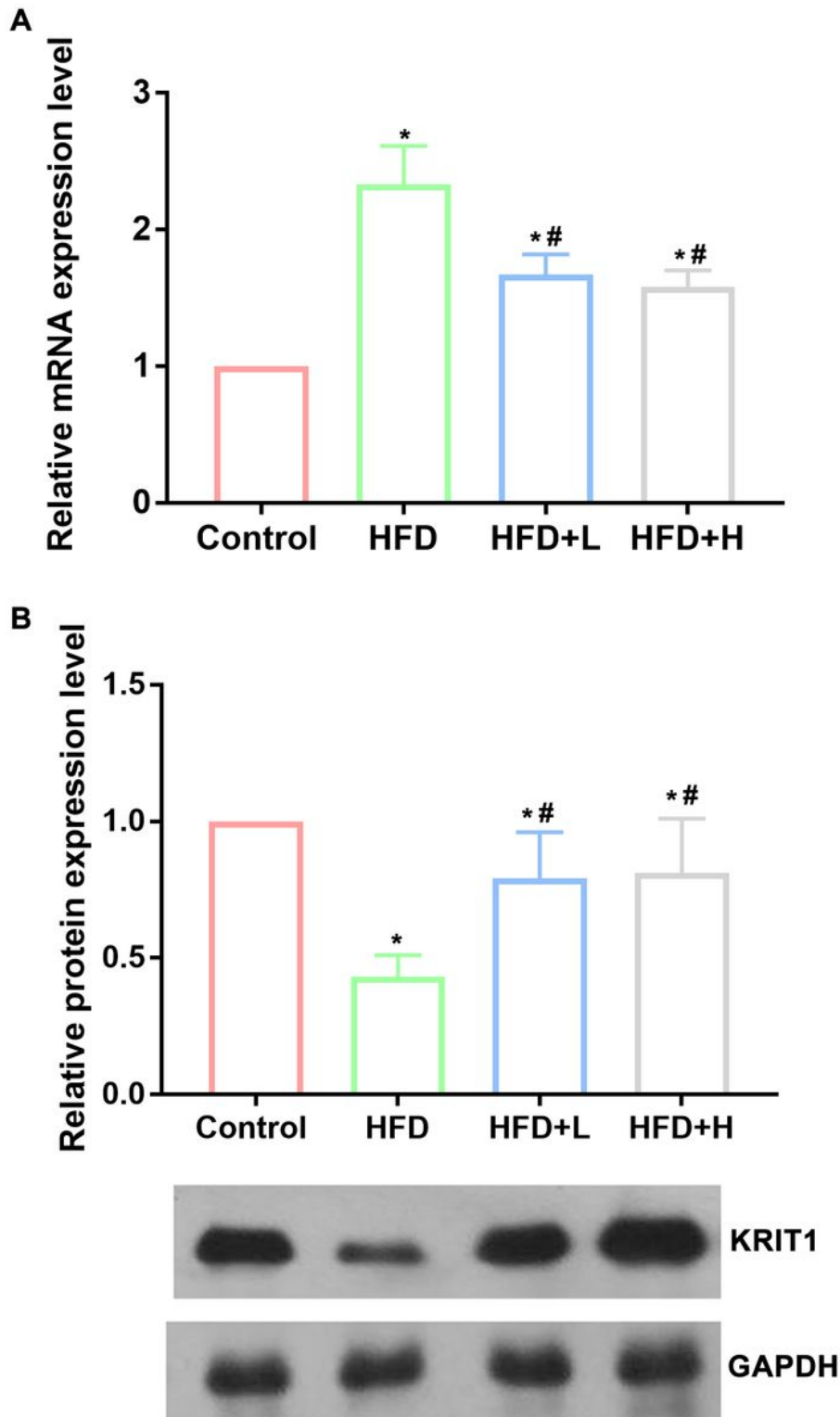


Figure 4

Effects of Rb1 administration on changes in miR-21-5p/KRIT1 axis in HFD rats. HFD rats were administrated with Rb1 of two doses (20 mg/kg BW and 40 mg/kg BW). The expression levels of miR-21-5p (A) and KRIT1 (B) were detected. “*” represented $P < 0.05$ vs. Control group. “#” represented $P < 0.05$ vs. HFD group. Each parameter was represented by three replicates.

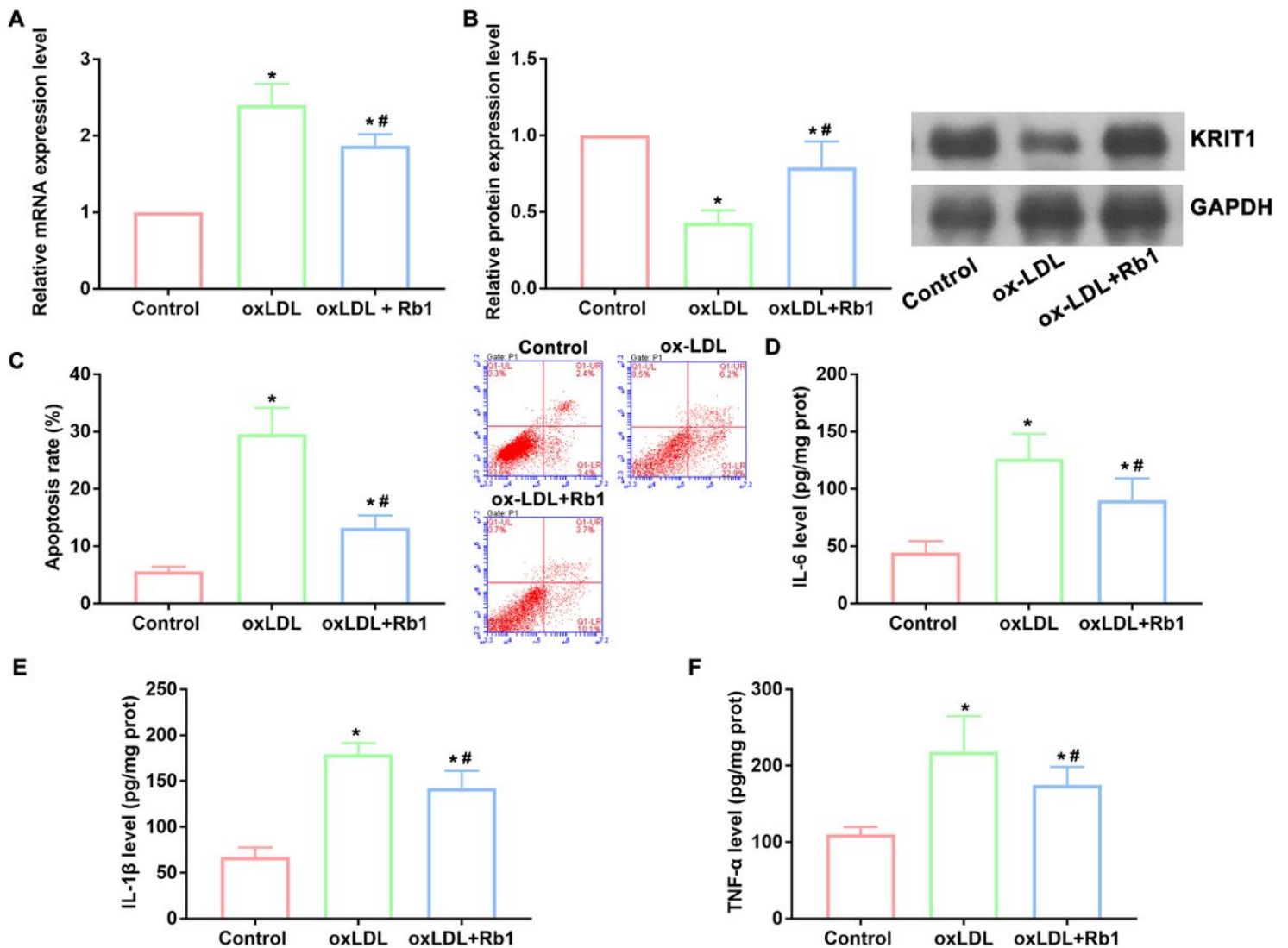


Figure 5

Effects of Rb1 on changes in miR-21-5p/KRIT1 axis, cell apoptosis, and production of cytokines in oxLDL-treated HUVECs. HUVECs were incubated with oxLDL and 30 μ M Rb1 for for 24 h. The expression levels of miR-21-5p (A) and KRIT1 (B), cell apoptotic rate (C), and the production of IL-6 (D), IL-1 β (E), and TNF- α (F) were detected. “*” represented $P < 0.05$ vs. Control group. “#” represented $P < 0.05$ vs. oxLDL group. Each parameter was represented by three replicates.

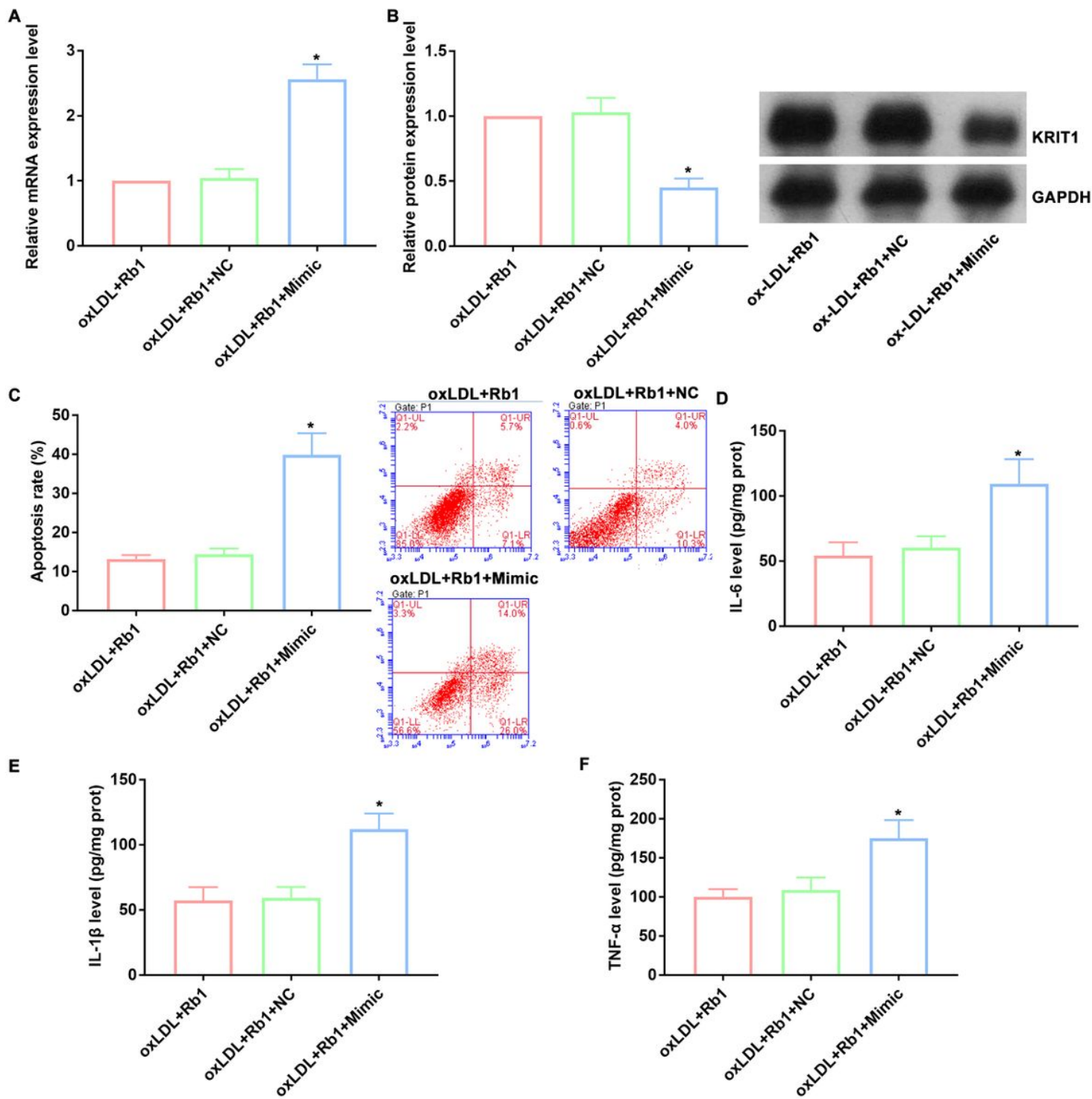


Figure 6

Effects of miR-21-5p mimic transfection on the protective effects of Rb1 against oxLDL-induced impairments in HUVECs. HUVECs were transfected with NC or miR-21-5p mimics, and then incubated with oxLDL and 30 μ M Rb1 for for 24 h. The expression levels of miR-21-5p (A) and KRIT1 (B), cell apoptotic rate (C), and the production of IL-6 (D), IL-1 β (E), and TNF- α (F) were detected. “*” represented P < 0.05 vs. ox-LDL+Rb1+NC group. Each parameter was represented by three replicates.

Supplementary Files

This is a list of supplementary files associated with this preprint. Click to download.

- [FigureS1.jpg](#)
- [Supplementaryfile.docx](#)